Numerical Methods in Civil Engineering

Hybrid Simulation of a Frame Equipped with MR Damper by Utilizing Least Square Support Vector Machine

Amir Hossein Sharghi *, Reza Karami Mohammadi ** and Mojtaba Farrokh ***

ARTICLE INFO

Article history:
Received:
October 2017.
Revised:
February 2018.
Accepted:
March 2018.

Keywords:
Hybrid simulation
Numerical simulation
MR damper
Hysteresis model
Least Square Support Vector Machine (LS-SVM)

Abstract:

In hybrid simulation, the structure is divided into numerical and physical substructures to achieve more accurate responses in comparison to a full computational analysis. As a consequence of the lack of test facilities and actuators, and the budget limitation, only a few substructures can be modeled experimentally, whereas the others have to be modeled numerically. In this paper, a new hybrid simulation has been introduced utilizing Least Square Support Vector Machine (LS-SVM) instead of physical substructures. With the concept of overcoming the hybrid simulation constraints, the LS-SVM is utilized as an alternative to the rate-dependent physical substructure. A set of reference data is extracted from appropriate test (neumerical test) as the input-output data for training LS-SVM. Subsequently, the trained LS-SVM performs the role of experimental substructures in the proposed hybrid simulation. One-story steel frame equipped with Magneto-Rheological (MR) dampers is analyzed to examine the ability of LS-SVM model. The proposed hybrid simulation verified by some numerical examples and results demonstrate the capability and accuracy of this new hybrid simulation.

1. Introduction

Currently, hybrid simulation has become more popular, especially in earthquake engineering, due to the advantages of this technique. In this method, the structure is divided into two main parts: The numerical (or finite element model) and the experimental (or physical) part. In this novel technique, the important parts that possess complex behavior are tested experimentally and the remaining structures which can be precisely modeled by finite element tools are modeled numerically. The users can perform accurate tests with affordable costs and acceptable focus on the main part by means of hybrid simulation. Combining the numerical and experimental part was executed in 1969 to introduce the concept of Pseudo-Dynamic test (Hakuno M 1969 [11]). From that point, many types of researches have been performed to develop and verify hybrid simulation (Takanashi and Nakashima 1987[23]) and (Mahin, Shing et al. 1989[15]).

Facilities play a key role in the execution of hybrid simulation. Therefore, insufficient facilities would restrict the usage of hybrid simulation exclusively to structures with limited substructures. In hybrid simulation, numerical and experimental errors cannot be eliminated under any circumstance. As indicated in Fig.1, the experimental setup introduces various sources of error in hybrid simulation that can have the most substantial influence on the simulation results. These errors include actuator tracking errors and controller tuning, calibration errors of instrumentation and noise generated in measurement instrumentation and A/D converters. Usually, numerical errors can be reduced beyond the desired precision for results by following certain modeling and analysis guidelines. The errors in experimental substructures can also be reduced by proper tuning and calibration of test equipment and using high-performance instrumentation, although it is virtually impossible to entirely eliminate the experimental errors.

** Ph.D. Candidate, Civil Engineering Department, K. N. Toosi University of Technology, Tehran, Iran.*
*** Corresponding author, Associate Professor, Civil Engineering Department, K. N. Toosi University of Technology, Tehran, Iran. E-mail: rkarami@kntu.ac.ir*
****Assistant Professor, Aerospace Engineering Department, K. N. Toosi University of Technology, Tehran, Iran.*

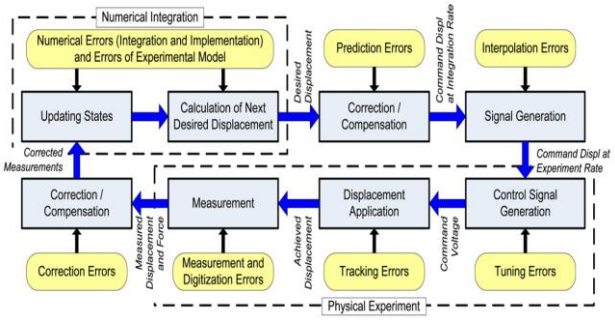

Fig. 1: Sources of error in hybrid simulation (Ahmadizadeh and Mosqueda, 2009[2]).

In feedback systems like hybrid simulation, even small errors can accumulate during the experiment and significantly alter the simulation outcome, yielding inaccurate or unstable results. This is due to the fact that in time-stepping integration algorithms, experimental measurements contaminated by errors are used to compute subsequent commands. Hence, it is imperative to recognize the most important sources of error in hybrid simulation and seek ways to minimize and compensate these errors (Ahmadizadeh and Mosqueda, 2009 [2]).

Model updating and hysteresis identification of substructures is a method for overcoming the limitation of hybrid simulation. Hysteresis is not a unique phenomenon or a one to one mapping problem. Updating hysteretic behavior (Yang, Tsai et al. 2012 [29]), material constitutive relationship (Elanwar and Elnashai 2016 [7]) and sectional constitutive models (Wu, Chen et al. 2016 [26]) of the experimental part include three approaches, all of which are deployed for calibrating the corresponding numerical substructures. Initially, Neural network is used as predictor of incremental forces on the specimen to achieve the displacement of the system (Zavala et al., 1996 [31]). In addition, it is also used for substructure online tests to predict the nonlinear hysteresis characteristics for shear frames (Yang and Nakano 2005 [28]). Combining neural network as an informational and mathematical model to achieve a more accurate response of beam to column connection was yet another attempt, to gain advantage of hybrid simulation (Yun, Ghaboussi et al. 2008 [30]). Multilayer feed-forward neural networks (MFFNNs) and NARX, as general approximator tools, are utilized for modeling and identification of hysteresis (Farrokh, Dizaji et al. 2015 [9]). By including additional variables, these systems can learn the one to many mapping problems like hysteresis in spite of incorporating some restrictions.

Farrokh (2018 [8]) proposed a new model for identification of the hysteretic behavior based on the learning capabilities of the LS-SVMs. The model first converts hysteresis, which is a multiple-valued nonlinearity, into a one-to-one mapping by means of the classical hysteresis stop operators similar to the Preisach model. Then the mapping is learned by an LS-SVM. Preisach model has superiority over the models and takes advantage of NARX-based since they cannot construct a complete memory for hysteresis and are prone to error accumulation due to the required feedback. In addition, it has some advantages over the neural-based hysteresis models because LS-SVMs have fewer problems in architecture determination and overfitting. Although this intelligent hysteresis model is mathematically equivalent to its origin, the Preisach model, practically can be applied more easily than the Preisach model owing to its LS-SVM part which acts as an intelligent tool.

In this paper, it has been shown that the improved pre-mentioned model can be successfully utilized instead of MR damper as substructure in hybrid simulation. The architecture of the input layer of the model has been improved for identification of MR dampers. LS-SVM can learn hysteresis model of material and with the concept of overcoming the hybrid simulation restrictions, LS-SVM will be utilized as an experimental substructure in hybrid simulations. By easing the assessment of proposed hybrid simulation, virtual hybrid simulations with the help of OpenSees and UI-SIMCOR (Kwon, Nakata et al. 2007 [14]) (as the coordinator software) are executed to investigate the new method. In this technique the reference data for training the LS-SVM is achieved from numerical models instead of experimental data. Consequently, the LS-SVM will perform the role of experimental substructures in hybrid simulation. Models of one story frames are designed to verify the ability of LS-SVM for hybrid simulation. The corresponding results exhibit the ability and accuracy of this new proposed hybrid simulation and demonstrate the high capability of the enhanced model for MR damper. The model for MR dampers are assessed as a substructure with different excitations, and the application of the model for MR damper is discussed. The results indicate the high ability of this proposed hybrid simulation.

2. Least square support vector machine (LS-SVM)

Supervised learning systems that analyze data and recognize patterns, known as support vector machines (SVMs), are used for classification (machine learning) and regression analysis. Support Vector Machines (SVMs) were introduced in 1992 (Boser, Guyon et al. 1992[3]). In this method, one maps the data into a higher dimensional input space and the other constructs an optimal separating hyperplane in this space (more information is available in "Least Square Support Vector machine by Suykens et al.") (Suykens, Van Gestel et al. 2002 [22]). The soft margin classifier was introduced by Cortes and Vapnik (1997 [5]), and later, the algorithm was extended to the case of regression by Vapnik (Vapnik, Golowich et al. 1997 [24]). SVMs can be used as linear and nonlinear classifiers as well as function approximators actually known as sparse kernels. The standard form of the SVMs adopts ε-insensitive loss function while LS-SVMs utilize squared loss function. In this version, one finds the solution by solving a set of linear equations instead of a convex quadratic programming (QP) problem for classical SVMs. Least squares SVM classifiers were proposed by Suykens and Vandewalle (1999 [21]). LS-

SVMs are a class of kernel-based learning methods. The main relations utilized to estimate the static function by LS-SVMs are presented in the following equations(Farrokh 2018[8]). First, the input data maps **z** to a high dimensional feature space by LS-SVM and approximates the output f through a linear regression by equation (1):

$$f(\mathbf{z}) = \mathbf{w}^{\mathrm{T}}\psi(\mathbf{z}) + b \tag{1}$$

Where **w** is a weight vector, b is the bias, and ψ (.) indicates a nonlinear mapping from the input space to a feature space. Equation (1) approximates the unknown nonlinear function $f=f(\mathbf{z})$. Assuming training data set $\{\mathbf{z}^m, f_m\}_{m=1}^{N}$ where N represents the number of training data set, its training can be expressed by the following optimization problem in the primal weight space:

$$\min_{\mathbf{w},b,\mathbf{e}} J_{\mathrm{p}}(\mathbf{w},\mathbf{e}) = \frac{1}{2}\mathbf{w}^{\mathrm{T}}\mathbf{w} + \gamma\frac{1}{2}\sum_{m=1}^{N} e_m^2 \tag{2}$$

Subject to

$$f_{\mathrm{m}} = \mathbf{w}^{\mathrm{T}}\psi(\mathbf{z}^{\mathrm{m}}) + b + e_{\mathrm{m}} \tag{3}$$

Where e_{m} is residual error

To solve the optimization problem, a Lagrangian function for the problem is considered as follows

$$\mathrm{L}(\mathbf{w},b,\mathbf{e};\boldsymbol{\alpha}) = J_{\mathrm{p}}(\mathbf{w},\mathbf{e}) - \sum_{m=1}^{N}\alpha_n\left(\mathbf{w}^{\mathrm{T}}\psi(\mathbf{z}^{\mathrm{m}}) + b + e_{\mathrm{m}} - y_{\mathrm{m}}\right) \tag{4}$$

Where α_{n} are Lagrange multipliers. Optimization problem from the primal form (feature space) is converted to the dual form by means of the Karush-Kuhn-Tucker conditions. By utilizing these conditions and eliminating the variables **w** and **e**, parameters α and b are obtained according to the following set of equations:

$$\begin{bmatrix} 0 & \mathbf{1}_N^{\mathrm{T}} \\ \mathbf{1}_N & \boldsymbol{\Omega} + \dfrac{\mathbf{I}}{\gamma} \end{bmatrix}\begin{bmatrix} b \\ \boldsymbol{\alpha} \end{bmatrix} = \begin{bmatrix} 0 \\ \mathbf{f} \end{bmatrix} \tag{5}$$

Where $\mathbf{f}^{\mathrm{T}} = [\mathrm{f}_1, \mathrm{f}_2, ..., \mathrm{f}_N]$, $\boldsymbol{\alpha}^{\mathrm{T}} = [\alpha_1, \alpha_2, ..., \alpha_N]$, $\mathbf{1}_N^T = [1, 1, ..., 1]$, and I is an identity matrix of size N. The vector α is called support vector and its components are $\alpha_{\mathrm{m}} = \gamma e_{\mathrm{m}}$, $m = 1, 2, N$ where γ represents the regularization factor. This factor controls the trade-off between weight and residual squared error terms in equation (2). By employing the kernel trick, the Gram matrix **Ω** is defined as follows:

$$\boldsymbol{\Omega}_{mn} = \psi(\mathbf{z}^m)^{\mathrm{T}}\psi(\mathbf{z}^n) = \mathrm{K}(\mathrm{z}^{\mathrm{m}}, \mathrm{z}^{\mathrm{n}}), \qquad m,n = 1,2,\ldots,N \tag{6}$$

where $K(.,.)$ denotes a predefined kernel function. The role of the kernel function is to avoid the explicit definition of the mapping $\psi(.)$. The resulting LS-SVM model for function approximation becomes

$$\mathrm{f}(\mathbf{z}) = \sum_{\mathrm{n}=1}^{\mathrm{N}}\alpha_m K(\mathbf{z},\mathbf{z}^m) + b \tag{7}$$

where α_{m} and b are the solution of the linear set (5). The solution is unique if the Mercer kernel is utilized (Murphy 2012 [17]). In this case, the Gram matrix **Ω** is positive definite.

The simplest form of kernels is

$$K(\mathbf{z},\mathbf{z}^m) = \mathbf{z}^{\mathrm{T}}\mathbf{z}^m \tag{8}$$

which converts LS-SVM to a linear regression. The Radial Base Function (RBF) kernel which is widely utilized in nonlinear function estimation has been used in this research as follows:

$$K(\mathbf{z},\mathbf{z}^m) = \exp\left(\frac{\left\|\mathbf{z}-\mathbf{z}^m\right\|}{\sigma^2}\right) \tag{9}$$

where $\|\cdot\|$ represents Euclidean distance and σ denotes width parameter. Both aforementioned kernels are Mercer; therefore, α_{n} and b can be uniquely determined by equation (5) for pre-assigned hyper-parameters σ and γ.

2.1. Prandtl neural network hysteresis model (PNN)

The numerical modelling of hysteretic behavior is challenging. To overcome this problem, Joghataie and Farrokh (2008 [18]) proposed Prandtl neural network based on the Prandtl Ishlinskii operator. Prandtl proposed to model the elastic-plastic behavior of materials with the following relation (Visintin 1994 [25]):

$$f(t) = \int_0^{\infty} w(r)\varepsilon_r[x(t)]dr \tag{10}$$

In equation (10) $w(r)$=density function; ε_r =elastic-plastic (stop) operator; r=yield point of stop operator; $x(t)$=input signal; and $f(t)$=output signal. For positive real values, the integration over r can be defined. Equation (10) is known as classical Prandtl–Ishlinskii model that is also called stop operator. The output is calculated by weighted summation of immense number of stop operators. A stop operator is illustrated in Figs. 2(a)-(b). In Fig. 2(a) the mass is connected to a spring with unit stiffness. The threshold friction force is assumed as r. Regarding the force applied to spring z (output variable) and displacement of A as x (input variable), the mechanism of stop operator can be defined. The stop operator in the Prandtl model is rate independent; as a result, the input-output diagram remains unaffected regardless of the rate of variation of the input. Thus, for representing the state of a stop operator, the relative extrema of the input is sufficient (Brokate and Sprekels 1996 [4]). Accurately, the memory of a stop operator is affected by a subset of the relative extrema according to the so-called *wiping out* or *deletion* property (Mayergoyz 1991[16]), where each stop operator generates a nested hysteresis loop. As shown in Fig. 2(b), each stop operator is odd symmetric

with respect to the center point of its own hysteresis loop (Joghataie and Farrokh 2008 [13]).

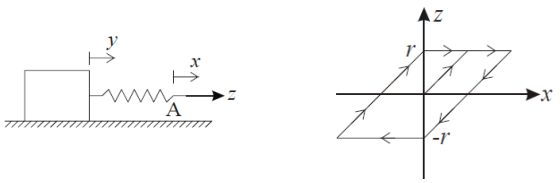

(a) Mechanism of stop operator (b) Hysteresis of stop operator

Fig. 2: Mechanism and hysteresis of Stop operator (Farrokh, Dizaji et al. 2015 [9])

The connection between the input and output signals of a stop operator can be represented by analytical form for piecewise monotonic input. By defining $t_i = i\Delta t$ and monotonic input in $[t_i, t_{i+1})$, equation (11) can be written as:

$$z(t) = \varepsilon_r[x(t)] \tag{11}$$

Where r is Prandtl parameter (yield point of stop operator) and ε_r as stop operator can be calculated by recurrence according to Eq. 12

$$\begin{aligned} z(t_{i+1}) &= \min\{r, \max\{-r, x(t_{i+1}) - x(t_i) + z(t_i)\}\} \\ z(0) &= x(0) = 0 \end{aligned} \tag{12}$$

2.2. LS-SVM hysteresis model

In this paper, preliminary model proposed by Farrokh (2018[8]) which is inspired by Preisach hysteresis that contains discrete hysteresis memory and multivariate function, is enhanced and a new version for modeling MR damper hysteresis is introduced. While Farrokh (2018[8])'s model was able to receive only one input, the new model proposed in this paper is capable of receiving two inputs, and the input for stop operator is unlike Farrokh (2018[8])'s model. At first, Farrokh (2018[8])'s model converts hysteresis into one-to-one mapping by stop operators (classical hysteresis operator), then the converted mapping is learned by LS-SVM. Details of the model is presented in Fig.3.

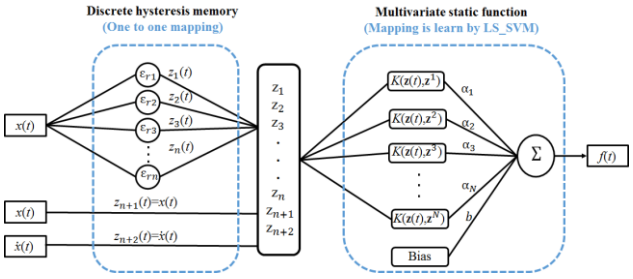

Fig. 3: LS-SVM hysteresis model architecture (2018[8])

The discrete hysteresis memory part consists of n stop operators with distinct threshold values r_1, r_2, …., r_n. These threshold values are assigned according to equation (13); where $|x|_{max}$ is the maximum of the input signal absolute values.

$$r_i = \frac{i}{(n+1)}|x|_{\max} \tag{13}$$

LS-SVM has been chosen for modeling the second part (multivariate static function) in order to estimate the memoryless functional ε_r in equation (11). Compared with the neural networks, LS-SVMs take advantage of the error functions with unique global minimum with respect to their weights. As mentioned earlier, training of the LS-SVM will be executed in one step through equation (5), with preassigned hyper-parameters γ and σ. High generalization ability of the model relies on the appropriate tuning of these hyper-parameters. The tuning process is performed in two successive stages: 1) Coupled Simulated Annealing (CSA) (Xavier-de-Souza, Suykens et al. 2010[27]) which determines suitable values for hyper-parameters and 2) Nelder-Mead simplex algorithm (Nelder and Mead 1965 [18]) which uses these previous values as starting values in order to perform a fine-tuning of the hyper-parameters. Afterwards, the training of LS-SVM is done with the optimum hyper-parameters on the training data. The tuning and training procedures in this study have been implemented by utilizing MATLAB LS-SVMlab Toolbox (Version 1.8) (De Brabanter, K., et al. 2011 [6]).

2.3. Utilizing the LS-SVM hysteresis model for different dampers

In this section, an explanation of steps for training and testing of dampers will be elaborated. An appropriate test is a test which covers the upper and lower bounds of displacement and velocity that has been experienced by sub-structure. The classification of damper should be initially done by putting them in rate-dependent or rate-independent group. Then, by considering the application of dampers, the ranges of their displacement and velocity have to be covered by utilizing proper excitations. For instance, the MR damper in one story building will experience 0.01 m and 0.4 m/s displacement and velocity, respectively. By considering the limits in the previous step, proper excitations are used for MR damper. Third, the suitable input for input layer and stop operator are chosen. Finally, with the help of MATLAB LS-SVMlab Toolbox (Version 1.8) (De Brabanter, K., et al. 2011 [6]), the training process is accomplished and if it is satisfactory then the model should be tested by other excitations; otherwise the excitation, input layer or some tuning parameters in LS-SVMlab Toolbox should be modified. In Fig. 4, the steps for utilizing LS-SVM hysteresis model for dampers are illustrated.

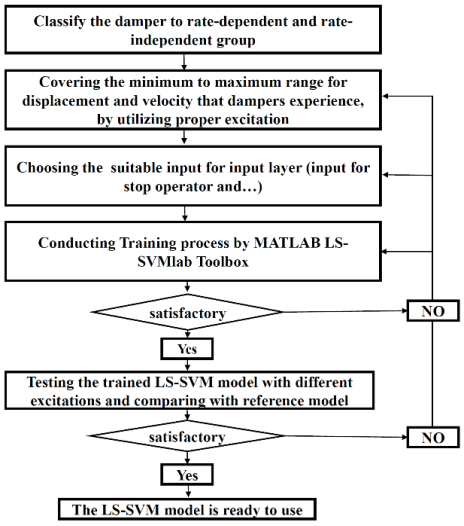

Fig. 4: Procedure of training and testing of LS-SVM hysteresis model

3. Magneto-rheological dampers (MR damper)

MR dampers are adaptable and reliable semi-active devices, which have a large force capacity but require low power levels to achieve them (Friedman, Zhang et al. 2010[10]). MR dampers are intrinsically nonlinear and rate-dependent devices. Therefore, preparing an efficient and accurate model for describing their behavior is a highly challenging task (Jiang and Christenson 2012[12]). Generally, the damper modeling is divided into parametric and nonparametric models. In the parametric models, the device is modeled as a collection of linear and nonlinear springs and dampers, then the corresponding parameters are expressed as mathematical equations. In the non-parametric method, the damper can be modeled with functions or ANN (artificial neural network) (Sapiński and Filuś 2003[19]).

3.1 Analytical Modeling of MR damper

The Spencer phenomenological model, one of the most popular models, has been chosen for simulation of MR damper (Fig. 5). The model is based on the response of a prototype MR damper which is obtained for evaluation from the Lord Corporation. The damper force of Spencer's model can be written by equation (14), where *z* and *y* are defined as equation (15) and (16), respectively. The model parameters depend on the voltage *V* as written in equation (17), where *u* represents the output of the first-order filter equation (18). The fourteen parameters for Spencer's model are defined in Table 1 (Spencer Jr, Dyke et al. 1997 [20]).

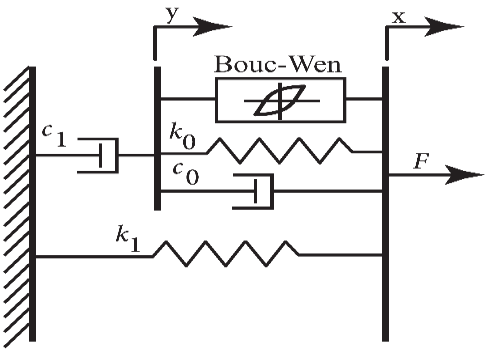

Fig. 5: Modified Bouc-Wen model for MR damper (Spencer Jr, Dyke et al. 1997 [20])

$$F = c_1\dot{y} + k_1(x - x_0) \tag{14}$$

$$\dot{z} = -\gamma|\dot{x} - \dot{y}||z|^{n-1} - \beta(\dot{x} - \dot{y})|z|^n + A(\dot{x} - \dot{y}) \tag{15}$$

$$\dot{y} = \frac{1}{(c_0 + c_1)}\left[\alpha z + c_0\dot{x} + k_0(x - y)\right] \tag{16}$$

$$\begin{aligned} \alpha &= \alpha(u) = \alpha_a + \alpha_b u \\ c_1 &= c_1(u) = c_{1a} + c_{1b}u \\ c_0 &= c_0(u) = c_{0a} + c_{0b}u \end{aligned} \tag{17}$$

$$\dot{u} = -\eta(u - V) \tag{18}$$

Table 1. Optimized parameters for the generalized model (Spencer Jr, Dyke et al. 1997 [20])

Parameter	Value	Parameter	Value
c_{0a}	0.21 N.s/m	α_a	1.40 N/m
c_{0b}	.035 N.s/m. V	α_b	6.95 N/m .V
k_0	0.469 N /m	γ	0.0363 m^{-2}
c_{1a}	2.83 N.s/m	β	0.0363 m^{-2}
c_{1b}	0.0295 N.s/m .V	A	301
k_1	0.05 N/m	n	2
x_0	0.143 m	η	190 s^{-1}

4. Assessment of LS-SVM hysteresis model for MR damper

In this section, the capabilities of the LS-SVM hysteresis model is evaluated for MR damper hysteresis applied input voltage. MR damper hysteresis is categorized in the rate-dependent group. In rate-dependent hysteresis, the output signal of the hysteretic system *y(t)* depends on the rate at which the input signal *x(t)* changes. For MR damper hysteresis, the shape is affected by $\dot{x}$ (velocity). The new proposed version LS-SVM hysteresis model which is used in this section, is illustrated in Fig. 6. For this model, $\dot{x}$ is input for Prandtl operator and *x(t)* and *V(t)*(voltage) are in input layer, while the output layer contains *F(t)* (MR damper force). For the first attempt, the *x(t)* was input for Prandtl operator but the result was not satisfactory and this model was chosen by trial and error.

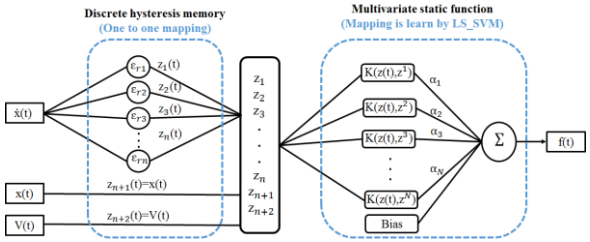

Fig. 6: Architecture of LS-SVM hysteresis model for MR damper

The input-output pairs were generated based on the data collected from the analysis of the one-story shear frame (m=10000N.s^2/m, k=146800 N/m) equipped with MR damper. MATLAB software was used to model the shear frame equipped with Spencer's numerical model (Spencer Jr, Dyke et al. 1997 [20]) for nonlinear dynamic analysis. The frame was subjected to 100% and 200% of white noise acceleration time history as illustrated in Fig. 7. White noise signal has been chosen to possess all the frequency content and covers the maximum of the velocity and displacement that MR damper will experience in the proposed structure for this study. Also the constant voltages shown in Fig. 8 were used in training process. Then pair data from two excitations was utilized for training the LS-SVM for modeling hysteresis.

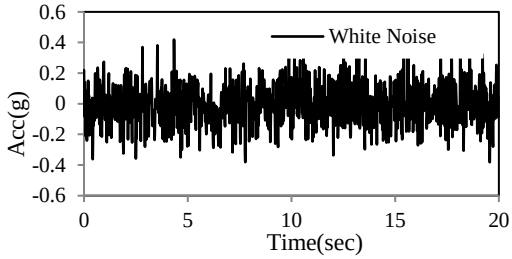

Fig. 7: White noise excitation for training

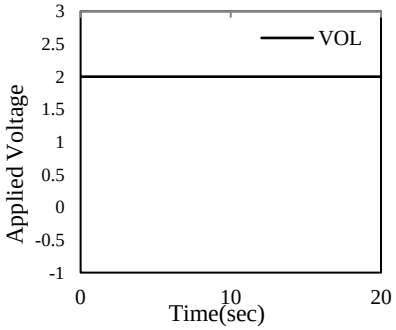

Fig. 8: Applied voltage, V=2

Figs. 9,10 displays the comparison of plot of reference (Spencer's numerical model) damper force versus velocity and the plot of hysteresis, with corresponding plot of the LS-SVM model, in which the trained systems were tested by the same white noise and voltage used for training. For training the LS-SVM, due to the advantage of not having to define the network architecture and the number of neurons (which was taken as fifteen), the training procedures were performed only once. Due to the ability of LS-SVM model, these systems confront fewer problems with architecture and number of neurons. In other words, the number of neurons do not have a specific effect on the accuracy of training process. In Table 2 the Root Mean Square of Errors (RMS_E) and relative error for the maximum force for LS-SVM in comparison with the reference model are illustrated. These are calculated based on the following equations:

$$RMS_E = \sqrt{\frac{\sum_{i=1}^{n}(X_{ref,i} - X_{model,i})^2}{n}} \quad (19)$$

$$Error = \frac{X_{ref,\max} - X_{model,\max}}{X_{ref,\max}} \quad (20)$$

in which, X_{ref}, i, and X_{model}, i represent damper forces in step i, in the reference model and the considered system, respectively. n, is the number of total steps. According to Figs. 9, 10 and Table 2, the LS-SVM ability for hysteresis modeling is acceptable.

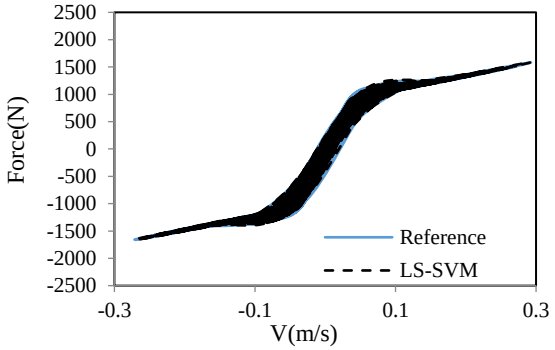

Fig. 9: Comparison of Reference (Spencer's model) and *LS-SVM* response (200% white noise)

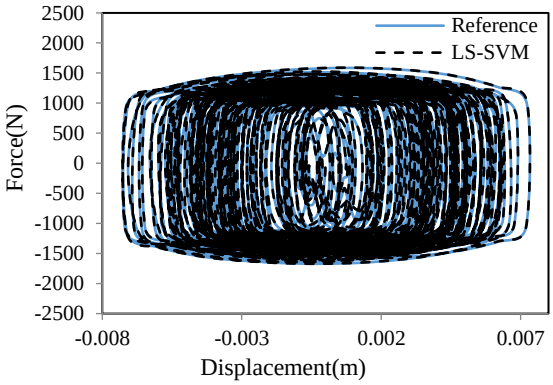

Fig. 10: Comparison of Reference (Spencer's model) and *LS-SVM* response (200% white noise)

Table 2. RMS_Es and relative errors of maximum force for different method (passive on) under 200% white noise

Response	Max-Force (N)	Err. (%)	RMS_E (N)
Reference	-1660.10	0	0
LS-SVM	-1661.85	0.105	12.14

5. Hybrid simulation for one-story frame equipped with MR damper

In this section, the detailed example on how to use a trained LS-SVM instead of a physical substructure (MR damper) will be studied. To conduct hybrid simulation, a 2-dimensional one-story steel frame which is illustrated in Fig. 11 is modeled using the computer program Open System for Earthquake Engineering Simulation (OpenSees). The height of the story and the span length for this building are selected to be 3 m and 4.2 m, respectively. The total nodal mass is equal to 16880N.s2/m. A standard double IPE180 is used for the columns. Double 100*100*10 mm angles were used for the bracing system. An MR damper was incorporated into the structure using a chevron bracing system.

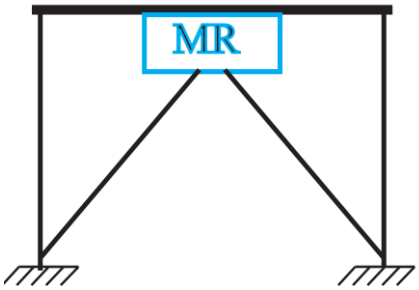

Fig. 11: Typical frame equipped with MR damper

The stress-strain behavior of steel was modeled with Hysteretic Material in OpenSees. Columns are modeled using nonlinear Beam-Column elements with fiber sections. Spread plasticity models are employed to model nonlinear behavior of column elements. The rigid beams are assumed to have the same displacement at the top nodes.

There are several software frameworks such as UI-SIMCOR, OPENFRESCO, MERCORY etc. For the purpose of hybrid simulation. Among them UI-SIMCOR is utilized for hybrid simulation in this study. The Multi-Site Substructure Pseudo-Dynamic Simulation Coordinator (UI-SIMCOR) was developed at the University of Illinois at Urbana-Champaign. This package uses a variety of communication protocols to integrate its numerical simulation with other analysis software or laboratory test equipment in local or remote sites (Ahmadizadeh 2007 [1]). Also, UI-SIMCOR is an open source public domain and is written in Matlab. LS-SVM model is defined as a function in Matlab and for every step of analysis, the displacement and velocity from UI-SIMCOR are sent as an input of LS-SVM model function.

The steel frame equipped with MR damper is divided into two parts as indicated in Fig. 12. The MR damper is selected as the physical substructure which should be replaced by the LS-SVM model. The rest of the structure with mass is considered as the numerical substructure which is modeled in OpenSees (OP-LS). In a parallel analysis, the MR damper is modeled by Spencer's (Spencer Jr, Dyke et al. 1997 [17]) model and the rest of the structure is modeled by Opensees (OP-SP) in Fig. 12 to provide a reference model to check the performance of trained LS-SVM model in proposed hybrid simulations.

The frame equipped with MR damper **with different voltage** (V=1) that was considered for training process (V=2) is subjected to **an excitation other than the white noise which is used for training LS-SVM**. The 1940 El Centro, 200% and Northridge earthquake records are considered as the new excitations for both hybrid simulations. The three excitations are shown in Table 3.

Table 3. Three Excitation records for hybrid simulations

Excitation	Year	Earthquake name	Station name	PGA
Excitation.1	1940	El Centro 100%	USGS station 0117	3.41 m/s^2
Excitation.2	1994	Northridge 100%	090 CDMG station 24278	5.75 m/s^2
Excitation.3	1940	El Centro 200%	USGS station 0117	6.82 m/s^2

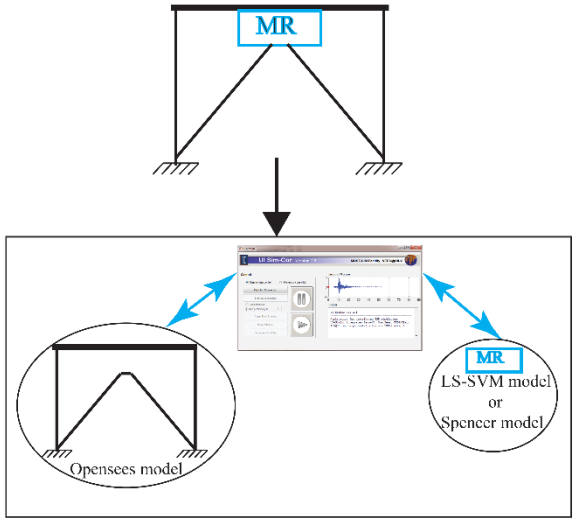

Fig. 12: Comparison of Reference (Spencer's model) (OP-SP) and *LS-SVM* response (OP-LS)

The results of the comparison of the reference and proposed hybrid simulation are illustrated in Fig. 13 to 18 for three excitations. Table 4 contains the RMSEs and relative error of maximum force for variable excitations. By comparing the figures and the error values, the high ability of the performance of proposed hybrid simulation is determined.

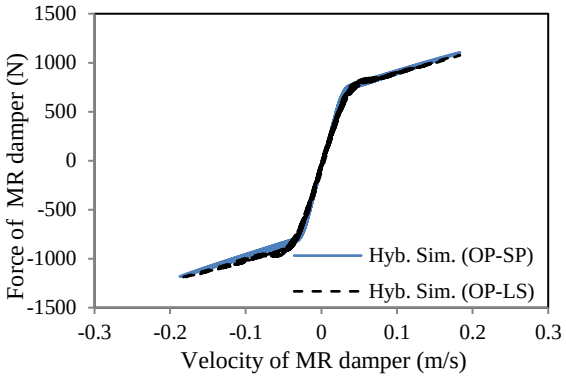

Fig. 13: Comparison of reference hybrid simulation (OP-SP)and (OP-LS) response (Excitation.1)

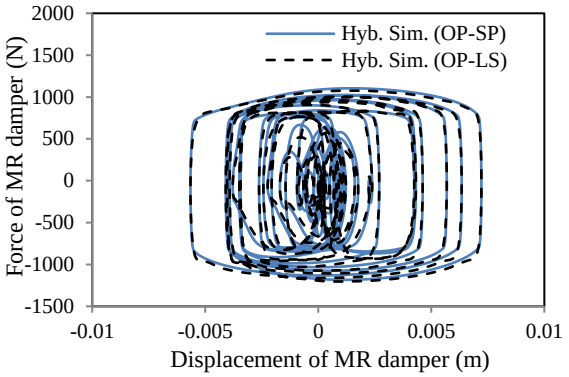

Fig. 14: Comparison of reference hybrid simulation (OP-SP)and (OP-LS) response (Excitation.1)

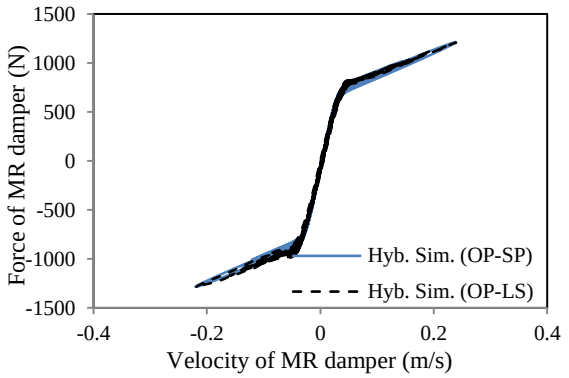

Fig. 15: Comparison of reference hybrid simulation (OP-SP)and (OP-LS) response (Excitation.2)

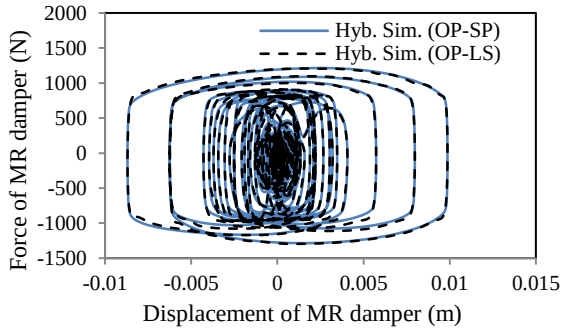

Fig. 16: Comparison of reference hybrid simulation (OP-SP)and (OP-LS) response (Excitation.2)

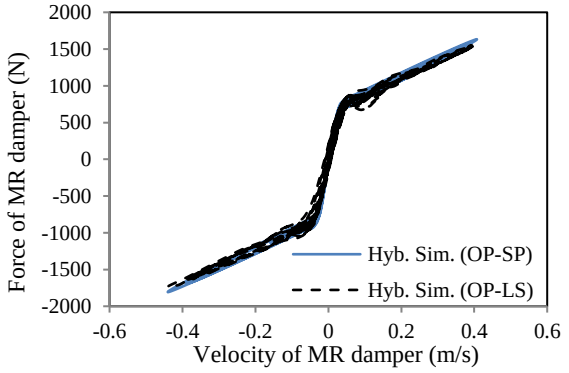

Fig. 17: Comparison of reference hybrid simulation (OP-SP)and (OP-LS) response (Excitation.3)

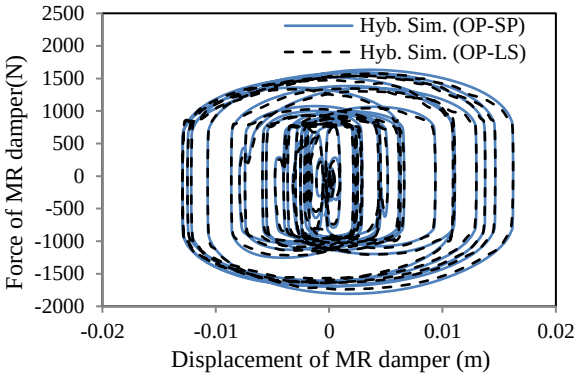

Fig. 18: Comparison of reference hybrid simulation (OP-SP)and (OP-LS) response (Excitation.3)

Table 4. RMS_Es and relative errors of maximum force under different excitations

	Response	Max-Force (N)	Err. (%)	RMS_E (N)
100% El Centro	***Reference***	-1183	0	0
	LS-SVM	-1161.9	1.78	54.84
Northridge	***Reference***	-1285.3	0	0
	LS-SVM	-1295	.75	29.76
200% El Centro	***Reference***	-1807.6	0	0
	LS-SVM	-1736.41	3.93	56.26

6. Conclusions

In this paper, new hybrid simulation was introduced. With regard to the proposed hybrid simulation, some physical substructures can be replaced by a suitably trained LS-SVM model. To execute this, after selecting the physical and numerical substructures and before performing the hybrid test, an appropriate test should be performed on the physical substructure to provide the inputs and outputs required for training the LS-SVM model. Consequently, the physical substructure can be replaced by the trained LS-SVM model even in the case that the structure is subjected to a different input excitation. Therefore, the trained LS-SVM model can play the role of substructure as a part of hybrid simulation without using the experimental setup. It was shown that LS-SVM model has a great ability to learn the hysteresis behavior of physical substructures (rate-dependent) with the training data achieved from dynamic test. By this method, it is possible to perform hybrid simulation for unlimited times and the trained LS-SVM model can be utilized for many substructures in different positions in one structure. The accuracy of proposed hybrid simulation was evaluated for one-story frame equipped by MR damper under different excitations. Based on the results of the verification examples used for assessment of LS-SVM model, the great ability of LS-SVM model and the feasibility of proposed method for improving the hybrid simulation are proven. In this paper, feasibility of proposed hybrid simulation has been testified through some numerical examples. However, the essence of performing hybrid simulation by experimental examples has been put aside for future rigorous study.

References

[1] Ahmadizadeh, M. Real-time seismic hybrid simulation procedures for reliable structural performance testing (PhD Dissertation), 2007. State University of New York at Buffalo.

[2] Ahmadizadeh, M. and Mosqueda, G., "Online energy-based error indicator for the assessment of numerical and experimental errors in a hybrid simulation." Engineering Structures, vol. 31(9), 2009, p. 1987-1996.

[3] Boser, B.E., Guyon, I.M. and Vapnik, V.N., "A training algorithm for optimal margin classifiers", In Proceedings of the fifth annual workshop on Computational learning theory, 1992, p. 144-152). ACM.

[4] Brokate, M. and Sprekels, J., "Hysteresis and Phase Transitions", vol. 121, 1996, Springer Science & Business Media.

[5] Cortes, C. and Vapnik, V., Lucent Technologies Inc, Soft margin classifier. U.S. 1997, Patent 5,640,492.

[6] De Brabanter, K., Karsmakers, P., Ojeda, F., Alzate, C., De Brabanter, J., Pelckmans, K., De Moor, B., Vandewalle, J. and Suykens, J.A., "LS-SVMlab toolbox user's guide: version 1.7", 2010, Katholieke Universiteit Leuven.

[7] Elanwar, H.H. and Elnashai, A.S., "Framework for online model updating in earthquake hybrid simulations", Journal of Earthquake Engineering, vol. 20 (1), 2016, p. 80-100.

[8] Farrokh, M., "Hysteresis Simulation Using Least-Squares Support Vector Machine", Journal of Engineering Mechanics, vol. 144(9), 2018, p.04018084.

[9] Farrokh, M., Dizaji, M.S. and Joghataie, A., "Modeling hysteretic deteriorating behavior using generalized Prandtl neural network", Journal of Engineering Mechanics, vol. 141(8), 2015, p.04015024.

[10] Friedman, A.J., Zhang, J., Phillips, B.M., Jiang, Z., Agrawal, A., Dyke, S.J., Ricles, J.M., Spencer, B.F., Sause, R. and Christenson, R., "Accommodating MR damper dynamics for control of large scale structural systems",In Proceedings of the Fifth World Conference on Structural Control and Monitoring, vol. 5, 2010, p. 10075).

[11] Hakuno, M., Shidawara, M. and Hara, T., "Dynamic destructive test of a cantilever beam, controlled by an analog-computer", In Proceedings of the Japan Society of Civil Engineers vol. 1969 (171), 1969, p. 1-9.

[12] Jiang, Z. and Christenson, R.E., "A fully dynamic magneto-rheological fluid damper model", Smart Materials and Structures, vol. 21(6), 2012, p.065002.

[13] Joghataie, A. and Farrokh, M., "Dynamic analysis of nonlinear frames by Prandtl neural networks", Journal of engineering mechanics, vol. 134(11), 2008, p. 961-969.

[14] Kwon, O.S., Nakata, N., Park, K.S., Elnashai, A. and Spencer, B., "User manual and examples for UI-SIMCOR v2. 6.", 2007, Department of Civil and Environmental Engineering, University of Illinois at Urbana-Champaign. Urbana, IL.

[15] Mahin, S.A., Shing, P.S.B., Thewalt, C.R. and Hanson, R.D., "Pseudodynamic test method—Current status and future directions", Journal of Structural Engineering, vol. 115(8), 1989, p. 2113-2128.

[16] Mayergoyz, I.D., "Mathematical Models of Hysteresis", 1991, Springer. New York.

[17] Murphy, K. P. (2012). "Machine learning: a probabilistic perspective." MIT Press, Cambridge, MA.

[18] Nelder, J.A. and Mead, R., "A simplex method for function minimizaion", The computer journal, vol. 7(4), 1965, p.308-313.

[19] Sapiński, B. and Filuś, J., "Analysis of parametric models of MR linear damper", Journal of Theoretical and Applied Mechanics, vol. 41(2), 2003, p.215-240.

[20] Spencer Jr, B.F., Dyke, S.J., Sain, M.K. and Carlson, J., "Phenomenological model for magnetorheological dampers", Journal of engineering mechanics, vol. 123(3), 1997, p.230-238.

[21] Suykens, J.A. and Vandewalle, J., "Least squares support vector machine classifiers", Neural processing letters, vol. 9(3), 1999, p. 293-300.

[22] Suykens, J.A., Van Gestel, T. and De Brabanter, J., "Least squares support vector machines", 2002, World Scientific.

[23] Takanashi, K. and Nakashima, M., "Japanese activities on on-line testing", Journal of Engineering Mechanics, vol. 113 (7), 1987, p. 1014-1032.

[24] Vapnik, V., Golowich, S. E and Smola, A. J., "Support vector method for function approximation, regression estimation and signal processing", Advances in neural information processing systems, 1997.

[25] Visintin, A, "Differential models of hysteresis", 1994, Springer Berlin.

[26] Wu, B., Chen, Y., Xu, G., Mei, Z., Pan, T. and Zeng, C., "Hybrid simulation of steel frame structures with sectional model updating Earthquake Engineering & Structural Dynamics, 45(8), 2016, p. 1251-1269.

[27] Xavier-de-Souza, S., Suykens, J.A., Vandewalle, J. and Bollé, D., "Coupled simulated annealing", IEEE Transactions on Systems, Man, and Cybernetics, Part B (Cybernetics), vol. 40(2), 2010, p. 320-335.

[28] Yang, W.J. and Nakano, Y., "Substructure online test by using real-time hysteresis modeling with a neural network", Advances in Experimental Structural Engineering, vol. 38, 2005, p. 267-274.

[29] Yang, Y.S., Tsai, K.C., Elnashai, A.S. and Hsieh, T.J., "An online optimization method for bridge dynamic hybrid simulations", Simulation Modelling Practice and Theory, vol. 28, 2012, p. 42-54.

[30] Yun, G.J., Ghaboussi, J. and Elnashai, A.S., "A new neural network-based model for hysteretic behavior of materials" International Journal for Numerical Methods in Engineering, vol. 73(4), 2008, p. 447-469.

[31] Zavala, C., Ohi, K. and Takanashi, K., "Neuro-Hybrid Substructuring On-Line Test on Moment Resistant Frames", In Proceedings of 11th World Conference on Earthquake Engineering, 1996, paper No. 1387.